Progress In Electromagnetics Research C, Vol. 21, 205–215, 2011

PLANAR W-BAND MIXER WITH A NOVEL IF-BLOCK

M. Zhan[1, *], Q. Xu[2], W. Zhao[1], Y. Zhang[1], R. Xu[1], and W. Lin[1]

[1]EHF Key Laboratory of Fundamental Science, University of Electronics Science and Technology of China, China

[2]China Defense Science & Technology Information Center, China

Abstract—A planar W-band single balanced mixer is designed and measured in this paper. This mixer is realized by using two novel IF-block, a rat-race ring with the fifth port, two beamlead GaAs Schottky diodes and two RF chokes. The novel IF-block which designed the first time in W-band is employed to provide reflection points for IF signal and to provide low loss path in wide bandwidth for the RF and LO signals. To our knowledge, the mixer shows the best conversion loss at 95 GHz and the highest 1 dB power compression ($P_{-1\,\mathrm{dB}}$) point among the W-band planar hybrid microwave integrated circuit (HMIC) mixers.

1. INTRODUCTION

Applications in W-band include radar, guidance, communication, radiometry, instrumentation, etc. With the rapidly growing demand for military and commercial applications, it has become increasingly important territory to be explored [1]. Compared to the waveguide structure mixers [2, 3], planar integrated technology has received considerable attention because of low cost (hybrid integrated circuit) and high performance (monolithic integrated circuit), especially in millimeter-wave bands [4–6].

In this paper, a low cost mixer is realized by using a configuration of two novel IF-blocks, a rat-race ring with the fifth port and two commercial Schottky diodes. The novel IF-block is based on parallel-coupled triple-line structure which can realize a stronger coupling coefficient than edge-coupled and end-coupled double-line

Received 24 February 2011, Accepted 10 May 2011, Scheduled 17 May 2011

* Corresponding author: Mingzhou Zhan (mzzhan@foxmail.com).

structure [7, 8], so wider bandwidth can be achieved under a certain line width and line spacing compared to the conventional double-line coupling structures. It has a low loss for the LO and RF signals and high rejection for the IF signal. The conversion loss of the mixer can be improved. The circuit design provides the advantages of low cost, small size, high performance and high reliability.

2. DESIGN AND DEVELOPMENT OF THE PLANAR W-BAND MIXER

Balanced mixers have inherent isolation between the LO and RF ports, the high 1 dB power compression point ($P_{-1\,\mathrm{dB}}$) of the RF signal. They also supply some rejection to certain spurious responses, LO noise and LO spurious signals. The only disadvantages are generally poorer conversion performance and larger LO power [3]. Basic designs for balanced mixers are mainly based on 90-degree and 180-degree hybrids. The 90-degree hybrid mixer is least used at microwave frequencies because this kind of mixer cannot be used as up-converter. The VSWR of RF port and the isolation between the LO and RF are poorer than 180-degree mixers and operate over a narrow frequency range compared with the rat-race mixer. In planar single balanced mixer design, 180-degree rat-race hybrid is commonly encountered. The LO signal is in phase, and the RF is 180° out of phase at the diodes, or vice versa, as shown in Fig. 1. This kind of configuration has no bonding wires or air bridges compared to the mixers in [6, 9, 10]. The RF is applied to the sigma port and the LO to the delta port of the hybrid. The two IF-blocks are used on the RF and LO lines to prevent the leakage of the IF signal. In this design, the IF-block is a triple-line structure

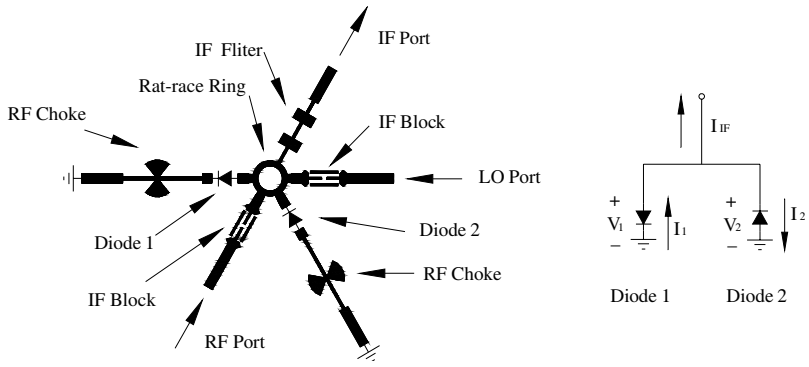

Figure 1. Configuration of the W-band rat-race mixer.

with small size, low insertion loss and wide bandwidth. The triple-line structure shows high coupling coefficient which can make the line width and line spacing requirement greatly relaxed for a specific coupling for wide band application. Then, the IF signals from the GaAs beamlead diodes (MA4E2037) are combined at the input of the lowpass filter (LPF) and filtered.

The current on the diode 1 can be expressed by the power series [11]:

$$I_1 = aV_1 + bV_1^2 + cV_1^3 + dV_1^4 + \ldots \tag{1}$$

$$V_1 = V_{LO}\cos(\pi + \omega_{LO}t) + V_{RF}\cos(\omega_{RF}t) \tag{2}$$

where V_1 is the total ac voltage across the diode 1, and I_1 is the current, and the lower-case letters represent constants.

The current on the diode 2 can be expressed by the power series:

$$I_2 = -aV_2 + bV_2^2 - cV_2^3 + dV_2^4 + \ldots \tag{3}$$

$$V_2 = V_{LO}\cos(\omega_{LO}t) + V_{RF}\cos(\omega_{RF}t) \tag{4}$$

where V_2 is the total ac voltage across the diode 2, and I_2 is the current. The lower-case letters represent constants. The IF current is as follow:

$$I_{IF} = I_1 - I_2 \tag{5}$$

The kth order spurious responses, those arising from mixing between $mf_{RF} + nf_{LO}$ where $m + n = k$, arise only the term of kth power in (1) and (3). All (m, n) spurious responses, where m and n are even, are eliminated. The $(2, 1)$ spurious response ($m = \pm 2,\ n = \pm 1$) is eliminated, but not the $(1, 2)$.

2.1. Design of the Rat-race Ring with the Fifth Port

The LPF in Fig. 2(b) is used to extract the IF signal and reject the LO and RF signals. The IF signal output filter has an ideal 50 Ohm impedance for IF signal and open-circuit impedance against the LO and RF signals, so the added fifth port for IF extraction will not affect the transmission property of the rat-race ring in the LO and RF frequency. Otherwise the phase and magnitude of the LO and RF signals on the diodes would be unbalance anymore and the mixer would have a poor conversion loss. Simulation and optimization of the hybrid ring is carried out in HFSS, the results are in Fig. 3 to Fig. 6.

The phase properties are shown in Fig. 3 and Fig. 4. The phase difference between the delta ports of the rings is $\Delta\theta_{LO}(f_{LO})$, and the phase difference between the sigma ports is represented by $\Delta\theta_{RF}(f_{RF})$, respectively.

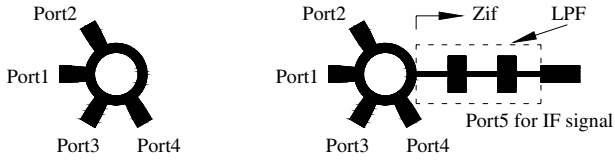

(a) rat-race hybrid (b) rat-race hybrid with LPF

Figure 2. Rat-race hybrid and rat-race hybrid with the fifth port.

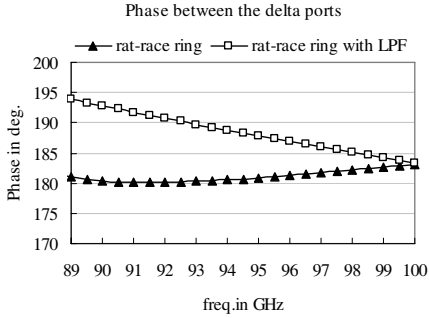

Figure 3. Phase properties of the two hybrids.

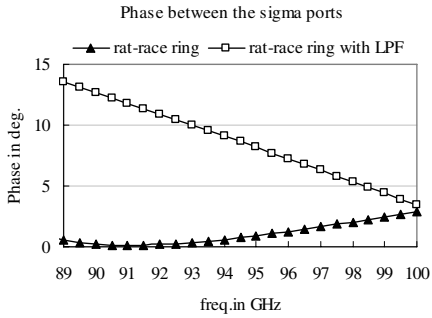

Figure 4. Phase properties of the two hybrids.

The normalized voltage on the diodes can be represented as:

$$\bar{V}_1 = -\frac{V_{LO1}}{V_{RF1}} \cos\left(\omega_{LO}t + \Delta\theta_{LO}\left(f_{LO}\right)\right) + \cos\left(\omega_{RF}t\right) \tag{6}$$

$$\bar{V}_2 = \frac{V_{LO2}}{V_{RF1}} \cos\left(\omega_{LO}t\right) + \Delta A_{RF2} \cos\left(\omega_{RF}t + \Delta\theta_{RF}\left(f_{RF}\right)\right) \tag{7}$$

Thus the phase difference of the IF signals ($\Delta\theta_{IF}$) between the diodes is:

$$\Delta\theta_{IF} = \left|\Delta\theta_{LO}\left(94GHz\right) - \Delta\theta_{RF}\left(f_{RF} \subseteq [89, 99]\right)\right| \leq 5^{\circ} \tag{8}$$

The single-balance mixer can be analyzed as two single-end mixers and an IF power combiner. The magnitude difference of the LO and RF signals is only 0.8 dB to 0.4 dB from 89 to 99 GHz. LO power ensures the "mixing state" of the diodes, it will not affects the conversion loss of each single-end mixer when LO is high enough. The magnitude difference of the RF ($\Delta A_{RF} \leq 0.8\,\mathrm{dB}$) in Fig. 5 will be transferred to the IF signals on each diodes when mixing. The IF signals are combined at the input port of the LPF, and the additional conversion loss (ΔL) caused by the phase and magnitude unbalance of the LO and

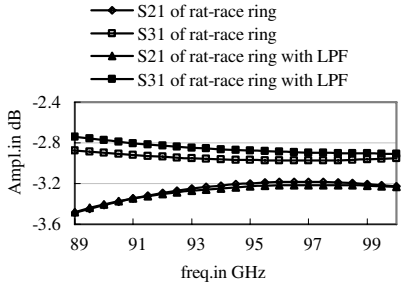

Figure 5. Insertion losses of the two hybrids.

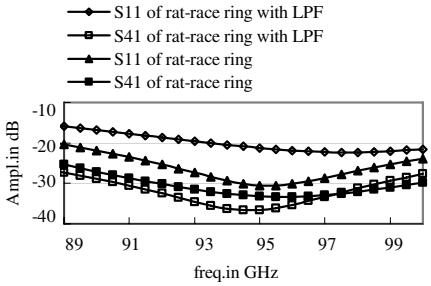

Figure 6. Isolation properties of the two hybrids.

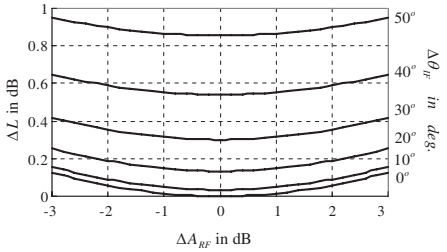

Figure 7. Relationship between ΔL and $\Delta\theta_{IF}$, ΔA_{RF}.

RF signals can be represented by (9). ΔL is plotted in Fig. 7, where $\Delta\theta_{IF}$ varies from 0° to 50°, and ΔA_{RF} varies from -3 dB to 3 dB. The unbalance of LO and RF does not have large impact on the conversion loss of the mixer, and the maximum ΔL of the W-band mixer is less that 0.1 dB in $89 \sim 90$ GHz.

$$\Delta L = 10 \log \left(\frac{1 + \Delta A_{RF}^2 + 2 \cdot \Delta A_{RF} \cdot \cos\left(\Delta\theta_{IF}\right)}{2 \cdot \left(1 + \Delta A_{RF}^2\right)} \right) \tag{9}$$

The isolation from LO to RF is about 21 dB at 94 GHz when the ports are all matched, as in Fig. 6. In real design, this parameter will be better or worse in several dB, because the diodes cannot be always matched to 50 Ohm from $89 \sim 99$ GHz.

2.2. Design of the Novel IF-block

IF-block is indispensable in this kind of rat-race hybrid mixer even the E-plan microstrip probe to waveguide transition is used as the output. There must be two reflection points to form open circuit on the LO and RF feeding points on the ring. Otherwise the conversion loss would deteriorate when working at high IF frequency.

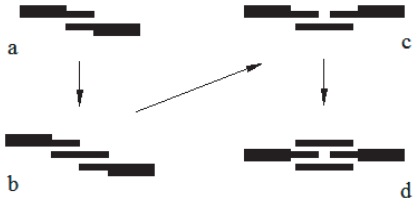

Figure 8. Evolution of the IF-block structure.

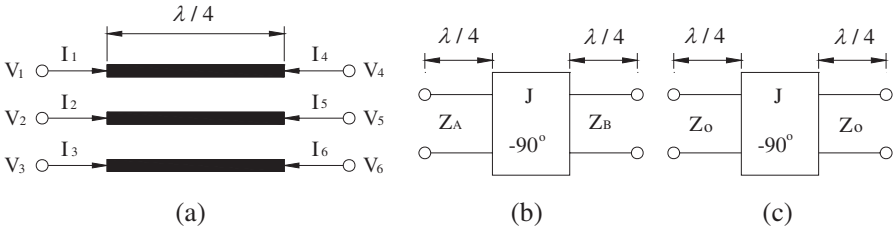

Figure 9. Analysis of the triple-line section.

An ideal IF-block must have low insertion loss for RF signal and high rejection for IF signal. In wideband application, bandwidth for RF signal is also important.

In Fig. 8, the evolution procedure of the IF-block is described, which is made out of a single cell of an edge coupled structure in Fig. 8(a); its bandwidth is constrained by the processing limitations of the line width and line spacing of the coupling section. The bandwidth of the structure in Fig. 8(a) can be improved in a straightforward manner at the expense of increasing the order of the coupled section, as in Fig. 8(b). Then the output port can be moved to the same side of the input port without changing the performance of the IF-block, as in Fig. 8(c). The IF-block proposed in this paper is evolved by simply adding a third line on the opposite side of the input line to increase the coupling, as in Fig. 8(d), so that the line spacing requirement can be relaxed for a specific coupling. Thus, the basic building block or coupled section for such a filter becomes a symmetric three-line microstrip structure in Fig. 9.

The analysis of the three-line coupled section mentioned in [7] is very useful. For the three-line structure, three quasi-TEM or dominant modes exist. By using the approach mentioned in [14, 15], the inductance matrix [L] and capacitance matrix [C] per unit length for the structure can be obtained. Since the structure is symmetric,

the eigenvoltage matrix for these dominant modes can be written as:

$$[M_V] = \begin{bmatrix} 1 & 1 & 1 \\ m_1 & 0 & -m_3 \\ 1 & -1 & 1 \end{bmatrix} \tag{10}$$

where $[M_V]$ is the eigenvoltage vector of the matrix product [L], [C]. The matrix $[M_V]$ is used to derive the relation between port voltages and port currents defined in Fig. 8(a) as:

$$\begin{bmatrix} V_a \\ V_b \end{bmatrix} = \begin{bmatrix} Z_a & Z_b \\ Z_b & Z_a \end{bmatrix} \cdot \begin{bmatrix} I_a \\ I_b \end{bmatrix} \tag{11}$$

where $[V_n] = [V_1, V_2, V_3]^T$, $[I_n] = [I_1, I_2, I_3]^T$, n is a or b, and the impedance matrices can be derived as in [13]:

$$[Z_n] = [M_V] \operatorname{diag}[-jZ_{mi} \cot \theta_i] [M_V]^T, \quad n = \ a \quad \text{or} \quad b \tag{12}$$

In (12), $\theta_i = \beta_i l$ with β_i is the phase constant of the ith mode, l is the length of the coupled section, and Z_{mi} is given by:

$$Z_{mi} = \frac{Z_{oi}}{mi^2 + 2} \tag{13}$$

where Z_{oi} is the characteristic impedance of mode i according to [13]. In (13), $m2 = 0$. According to [7] the network can be simplified to a two-port network. The approximations used in [13] are then to establish the equivalence inverter circuits in Figs. 9(b) and 9(c). The three modal phase constants are assumed to be approximately the same, and let $\beta_i l = \pi/2$ at the centre frequency. Comparing the two-port Z-parameters of the circuits in Fig. 9(a) with those in Fig. 9(b), it can be obtained that:

$$m1 \cdot Z_{m1} - m3 \cdot Z_{m3} = JZ_A Z_B \tag{14a}$$

$$m1^2 \cdot Z_{m1} + m3^2 \cdot Z_{m3} = Z_A \left(J^2 Z_A Z_B + 1\right) \tag{14b}$$

$$Z_{m1} + Z_{m3} = Z_B \left(J^2 Z_A Z_B + 1\right) \tag{14c}$$

The admittance inverter in Fig. 9(b) can be further approximated by the circuit in Fig. 9(c) with $Z_o^2 = Z_A Z_B$. To realize this, the product of (14b) and (14c) is reduced through taking the following approximation:

$$m1^2 + m3^2 = 2m1 \cdot m3 \tag{15}$$

Then the following approximation can be obtained:

$$m1 \cdot Z_{m1} + m3 \cdot Z_{m3} \approx Z_o \left(J^2 Z_o^2 + 1\right) \tag{16}$$

The key steps, which can greatly simplify the procedure to determine the line width and the line spacing of each coupled section in

a three-line bandpass filter, are (14a), (15) and (16) in this formulation. From the design equations for a bandpass filter in [12], the value of JZ, for each admittance inverter can be determined from the values of lumped circuit elements of the lowpass filter prototype. Once JZ is known, (14a) and (15) can be solved simultaneously to determine the values of $m1 \cdot Z_{m1}$ and $m3 \cdot Z_{m3}$ for each coupled section:

$$m1 \cdot Z_{m1} = (Z_o/2)\left(J^2 Z_o^2 + JZ_o + 1\right) \tag{17}$$

$$m3 \cdot Z_{m3} = (Z_o/2)\left(J^2 Z_o^2 + JZ_o + 1\right) \tag{18}$$

$m1 \cdot Z_{m1}$ and $m3 \cdot Z_{m3}$ in three-line coupled section play the same roles as $Z_{oe}/2$ and $Z_{oo}/2$ play in a two-line coupled section. Z_{oe} and Z_{oo} are the even-mode and odd-mode characteristic impedances, respectively, for a pair of coupled microstrip lines. It is known that the coupling coefficient C of a coupled two-line section of quarter wavelength can be written as [12]:

$$C = \frac{Z_{oe}/2 - Z_{oo}/2}{Z_{oe}/2 + Z_{oo}/2} \tag{19}$$

So the coupling coefficient K of a three-line section can be defined as:

$$K = \frac{m1 \cdot Z_{m1} - m3 \cdot Z_{m3}}{m1 \cdot Z_{m1} + m3 \cdot Z_{m3}} \tag{20}$$

When the substrate is chosen, we can use the K to design the line width and the line spacing of the filter. Based on the design method introduced above, the initial values of the filter in Fig. 8 can be obtained and optimized in HFSS to make sure the bandwidth as wide as possible, and the line width and the line spacing is 0.08 mm, which is the extreme dimension guaranteed by wet chemical etching process. It is fabricated on the 5 mil height Rogers 5880 substrate. The three-line IF-block structure exhibits a wide 1 dB-passband bandwidth of 36 GHz (about 40% of the center frequency), and the rejection for IF frequency is far more than 30 dB below 10 GHz, as in Fig. 10.

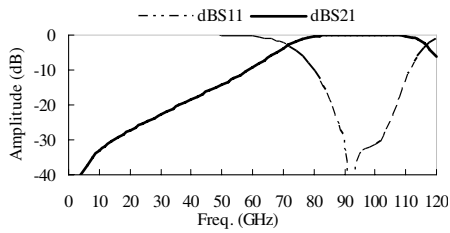

Figure 10. Simulated wideband response of the W-band IF-block.

3. SIMULATION AND MEASUREMENTS OF THE PLANAR W-BAND MIXER

The mixer in this paper is fabricated on a 5 mil Rogers 5880 substrate by using both circuit simulation and full-wave electromagnetic analysis to ensure the yielding. Fig. 11 shows the photograph of the mixer, and its size is $24 \times 24 \times 19\,\text{mm}^3$. The waveguide to microstrip transitions of the LO and RF ports, rat-race hybrid with the LPF, LO and RF chokes and triple-line IF-blocks are simulated in HFSS, then the S parameters of these components are imported into advanced design system (ADS) to simulate with the diodes using harmonic balance simulator.

The block diagram and instruments used to measure the mixer are shown in Fig. 12. Fig. 12(a) is used for measuring the conversion

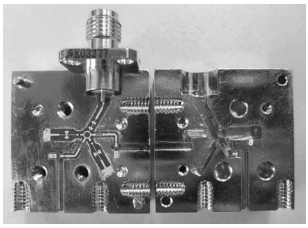

Figure 11. Photograph of the W-band rat-race mixer.

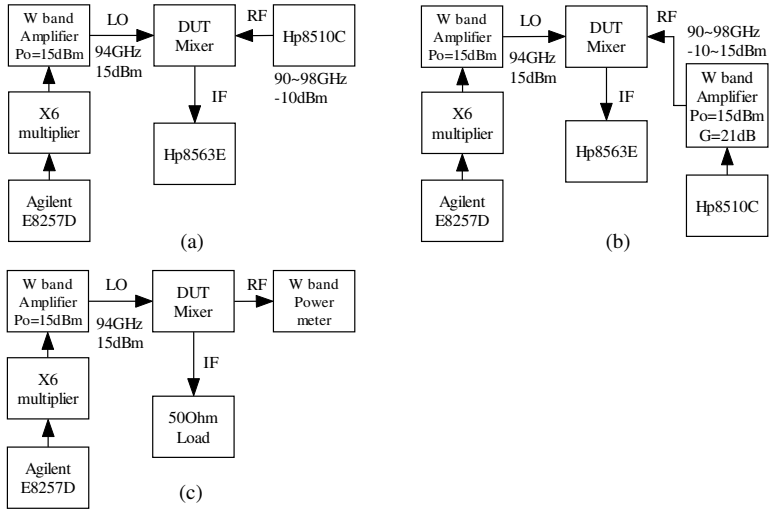

Figure 12. Block diagram for measurement. (a) block diagram for RF VSWR and conversion loss measurement, (b) block diagram for P-1 dB measurement, (c) block diagram for isolation measurement.

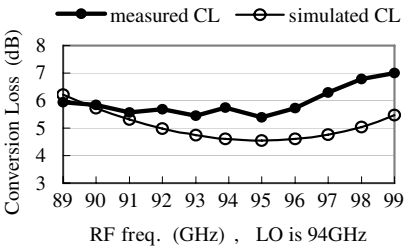

Figure 13. Measured and simulated conversion loss.

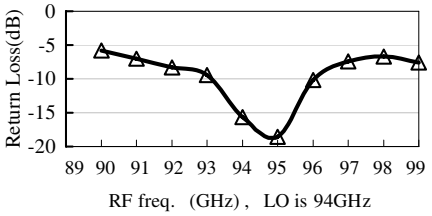

Figure 14. Measured return loss of RF port.

loss and return loss of the mixer. Fig. 12(b) is for the $P_{-1\,\mathrm{dB}}$, and Fig. 12(c) is for measuring the isolation from LO to RF port.

The simulated and measured conversion losses are presented in Fig. 13, the measured return loss of RF port is shown in Fig. 14. The measured $P_{-1\,\mathrm{dB}}$ is better than 10 dBm, and the measured LO-RF isolation is 26 dB when IF port is terminated by a 50 Ohm load. The LO power can be reduced by using lower barrier diodes or bias technology. As a consequence, the $P_{-1\,\mathrm{dB}}$ will be lower.

4. CONCLUSION

A planar W-Band mixer has been designed and measured in this paper. Based on the 5-port ring, the mixer has no cross jump-line in the topology, so it can be used in high IF situation with a low conversion loss. In addition, the novel wideband low-loss IF-block ensures the low transmission loss of the RF path, and then the conversion loss of the mixer is reduced. The measured conversion loss of the mixer is below 6.8 dB in 89 $\sim$ 99 GHz. The minimum conversion loss is 5.29 dB at 95 GHz which is the lowest specification in the HMIC planar mixer in W band as we have known. The RF input $P_{-1\,\mathrm{dB}}$ is 10 dBm. The LO to RF isolation is 26 dB, and the return loss at RF port is better than -5.8 dB in 89 $\sim$ 99 GHz range. Its size is $24 \times 24 \times 19\,\mathrm{mm}^3$.

REFERENCES

1. Tahim, R. S., G. M. Hayashibara, et al., "Design and performance of W-band broad-band integrated circuit mixers," *IEEE Trans. Microwave Theory & Tech.*, Vol. 31, No. 3, 277–283, 1983.
2. Bui, L. and D. Ball, "Broadband planar balanced mixers for millimeter-wave applications," *IEEE MTT-S Dig.*, 204–205, 1982.
3. Chang, K. and D. M. English, "W-band (75–110 GHz) microstrip

components," *IEEE Trans. Microwave Theory & Tech.*, Vol. 33, No. 12, 1375–1382, 1985.

4. Lee, Y.-C., C.-M. Lin, S.-H. Hung, C.-C. Su, and Y.-H. Wang, "A broadband doubly balanced monolithic ring mixer with a compact intermediate frequency (IF) extraction," *Progress In Electromagnetics Research Letters*, Vol. 20, 175–184, 2011.
5. Lin, C.-M., Y.-C. Lee, S.-H. Hung, and Y.-H. Wang, "A 28–40 GHz doubly balanced monolithic passive mixer with a compact IF extraction," *Progress In Electromagnetics Research Letters*, Vol. 19, 171–178, 2010.
6. Chien, W.-C., C.-M. Lin, Y.-H. Chang, and Y.-H. Wang, "A 9–21 GHz miniature monolithic image reject mixer in 0.18-μm Cmos technology," *Progress In Electromagnetics Research Letters*, Vol. 17, 105–114, 2010.
7. Kuo, J.-T. and E. Shih, "Wideband bandpass filter design with threeline microstrip structures," *IEE Proceedings Microwaves, Antennas and Propagation*, Vol. 149, No. 56, 243–247, 2002.
8. Tounsi, M. L., R. Touhami, A. Khodja, and M. C. E. Yagoub, "Analysis of the mixed coupling in bilateral microwave circuits including anisotropy for Mics and Mmics applications," *Progress In Electromagnetics Research*, Vol. 62, 281–315, 2006.
9. Rhee, J.-K. and S.-C. Kim, "3-D 94 GHz single balanced mixer using MHEMT and DAML technology," *34th International Conference on Infrared, Millimeter, and Terahertz Waves*, 1–4, Busan, 2009.
10. Matsuura, H. and K. Tezuka, "Monolithic rat-race mixers for millimeter waves," *IEEE Trans. on Microwave Theory & Tech.*, Vol. 46, No. 6, 839–841, 1998.
11. Mass, S. A., *Microwave Mixers*, 2nd Edition, Artech House, 1993.
12. Pozar, D. M., *Microwave Engineering*, 2nd Edition, John Wiley & Sons, New York, 1998.
13. Paul, C. R., *Analysis of Multi-conductor Transmission Lines*, John Wiley & Sons, New York, 1994.
14. Schwindt, R. and C. Nguyen, "Spectral domain analysis of three symmetric coupled lines and application to a new bandpass filter," *IEEE Trans. on Microwave Theory & Tech.*, Vol. 42, No. 7, 1183–1189, Jul. 1994.
15. Kuo, J. S., "Accurate quasi-TEM spectral domain analysis of single and multiple coupled microstrip lines of arbitrary metallization thickness," *IEEE Trans. on Microwave Theory & Tech.*, Vol. 43, No. 8, 1881–1888, Aug. 1995.